Int. J. Heat Mass Transfer. Vol. 23, pp. 1105–1115
Pergamon Press Ltd. 1980. Printed in Great Britain

0017–9310/80/0801–1105 $02.00/0

EFFECT OF RADIAL ELECTRIC FIELD ON HEAT AND MOMENTUM TRANSFERS IN DIELECTRIC ORGANIC LIQUID FOR LAMINAR FLOW THROUGH CONCENTRIC ANNULI

T. MIZUSHINA, F. OGINO, T. MATSUMOTO, M. YOKOYAMA and N. KITANO
Department of Chemical Engineering, Kyoto University, Kyoto, Japan 606

(*Received* 15 *October* 1979)

Abstract—Experiments were conducted to investigate changes in convective heat transfer in flows of dielectric organic liquids in annuli between copper tube and concentric wires. Also investigated was longitudinal pressure drop in the flow which could be induced by applying electric fields of direct current between the wall of the tube and the central wire electrode. In the laminar range of Reynolds number, heat transfer rates at the outer wall increased in the thermally well-developed region, and the thermal development was advanced. On the other hand, pressure drops were also increased in liquids of small Prandtl number. In the transitional and turbulent range, however, neither changes of heat nor momentum transfer were noticeable. To express these results in the low Reynolds number range a semi-empirical formulation in non-dimensional terms was derived from the similarity principle.

NOMENCLATURE

A_n, dimensionless constants in eigenvalue problem;
b, ion mobility [$m^2 V^{-1} s^{-1}$];
b^*, ion mobility of space-charge [$m^2 V^{-1} s^{-1}$];
c_p, specific heat of fluid at constant pressure [$J kg^{-1} K^{-1}$];
D_{eq}, equivalent diameter of annulus, $2(r_0 - r_i)$ [m];
$\mathscr{D}$, diffusivity of ion [$m^2 s^{-1}$];
$\mathscr{D}^*$, diffusivity of space-charge [$m^2 s^{-1}$];
$\mathbf{E}$, vector of electric field strength [$V m^{-1}$];
Es, dimensionless complex defined in equation (12);
en, density of space-charge [$A s^{-1} m^{-3}$];
$\mathbf{F}$, dimensionless vector of electric field strength, $[\mathbf{E}(\varepsilon b^* I_0 r_0)^{1/2}]$;
f, friction factor;
$\mathbf{I}$, flux of space-charge, total current density [$A m^{-2}$];
Gz, Graetz number $[(Z/D_{eq})/RePr]$;
l, length of test section [m];
N, dimensionless density of space-charge $[en(r_0 b^*/I_0\varepsilon)^{1/2}]$;
$N_\#$, value of N at $r_\#$;
Nu, Nusselt number $[q_0 D_{eq}/(T_b - T_0)\lambda]$;
P, dimensionless pressure $[pr_0^2\rho/\mu^2]$;
Pr, Prandtl number $[c_p\mu/\lambda]$;
p, pressure [$N m^{-2}$];
q_o, heat flux at outer wall [$J m^{-2} s^{-1}$];
Re, Reynolds number $[2(1 - r^*)\langle v_z\rangle]$;
$R_n(r)$, eigenfunctions;
r, radial distance [m], normalized by r_o[—];
$r_\#$, dimensionless radial position taking $N = N_\#$;
r^*, r_i/r_o;
r_o^+, Reynolds number based on friction velocity and tube radius;
T, temperature [K];
t, time [s];
V, electric voltage [V];
$V_\#$, voltage appearing in equation (11) [V];
$\mathbf{u}$, vector of velocity [$m s^{-1}$];
$\mathbf{v}$, dimensionless vector of velocity, $\mathbf{u}\rho r_o/\mu$;
$\langle v_z\rangle$, dimensionless space-averaged velocity, $\langle u_z\rangle\rho r_o/\mu$;
z, axial distance [m], normalized by r_o[—].

Greek symbols

Θ, dimensionless temperature difference from T_e, $[(T - T_e)\lambda/q_o r_o]$;
$\Theta_{\infty z}$, dimensionless temperature in the fundamental solution;
$\Theta_{\infty r}$, dimensionless temperature in the fundamental solution;
β, dimensionless constant in equation (11);
ε, dielectric constant of fluid [$A s V^{-1} m^{-1}$];
ε_M, eddy diffusivity of momentum [$m^2 s^{-1}$];
ε_H, eddy diffusivity of heat [$m^2 s^{-1}$];
μ, viscosity of fluid [$kg m^{-1} s^{-1}$];
ν, kinematic viscosity of fluid [$m^2 s^{-1}$];
λ, thermal conductivity of fluid [$J m^{-1} s^{-1} K^{-1}$];
λ_n, eigenvalues;
ρ, density of fluid [$kg m^{-3}$];
σ, dimensionless constant in equation (29);
τ, dimensionless time, $t\mu/\rho r_o^2$.

Subscripts

b, bulk condition;
e, inlet condition;

i, at central wire condition or component i;
o, at outer wall surface;
r, radial component;
z, axial component;
∞, fully developed.

1. INTRODUCTION

WHEN a fluid is subjected to high electric fields, a convection resulting from a momentum exchange between fluid partially charged particles and adjacent fluid occurs. This phenomenon is known as an ionic wind which is systematically discussed by Stuetzer [1, 2]. Also, an electrostrictive convection will occur by an interaction between the electrical and thermal field, owing to the temperature dependence of the dielectric constant. These effects on the natural convective heat transfer have been investigated since Senftleben [3] discussed the electrostrictive effects. The transfer rates have been found to increase by several times as much as pure natural convective ones. Kronig and Schwarz [4] substantiated the Senftleben effect around a thin heated wire forming an electric field with a cylinder. Frank [5], Yabe *et al.* [6] and Konno *et al.* [7] treated the ionic wind effects on natural convection of air around plates and cylinders, where the wind produced between the heat-transfer surface and needles or wires gave rise to a disturbance in the original convective fields.

As for the forced convection processes, similar studies were conducted by Moss and Grey [8] and Lazarenko *et al.* [9] in laminar flow of gases in tubes, and by Sadek *et al.* [10] and Velkoff and Godfrey [11] in laminar boundary layer flows of air. Mizushina *et al.* [12] applied an electric field to an air flow and showed that the ionic wind associated with the original forced flow induced either transitional or turbulent flow, even if Reynolds number were in the laminar region, and that heat transfer rates at the outer wall and longitudinal pressure drops increased considerably. But the electrostrictive effect was negligibly small and also the ionic wind effect decreased in the highly turbulent region. Robinson [13] dealt with heat transfer at the inner wire.

In considering forced convective liquids flow subjected to the electric field, similar phenomena to those in gas flow can be anticipated. In the case of liquids the flows are occasionally laminar and also the Prandtl number is so large that contributions of turbulent-like motion, even if the motion is small, to the mechanism of heat transfer may be large. After the pioneer work of Schmidt and Leidenfrost [14], Porter *et al.* [15, 16] discussed liquid flow of an insulating oil. However, more experimental work is desired in order to understand the behaviour of heat transfer under the electric field and to correlate the data, because only one kind of liquid was used in their experiments and Reynolds numbers are in narrow range.

The present paper shows the results of experimental investigations of electroconvective effects on three kinds of liquids flowing in concentric annuli.

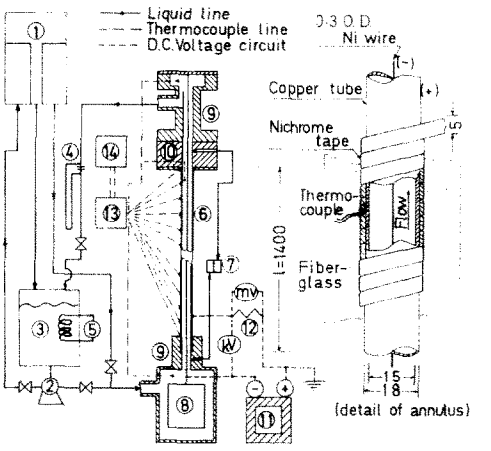

FIG. 1. Layout of experimental apparatus.

2. EXPERIMENTAL APPARATUS AND MEASUREMENTS

A configuration of the experimental apparatus is shown in Fig. 1. From a head tank process fluid flows into the bottom of a test section standing vertically, and returns through an orifice meter to a storage tank maintained at constant temperature. The test heat exchanger is a copper tube of 18 mm O.D. and 15 mm I.D., on which a nichrome tape of 5 mm width as a heat source is rolled. Both outlet and inlet tube header were fabricated from acrylic resin. At the center of the tube, a nickel wire of 0.3 mm dia. is strained by a weight of about 4 kg. Electric potentials of direct current were applied between the copper tube, which is maintained at earth potential, and the central wire, at a negative potential.

Electric currents through the annular space between the electrodes were measured by the voltage drop in a reference resistance of 10 kΩ (or 100 kΩ) connected in series to the high voltage circuit.

Heat generated in the nichrome tape was nearly completely transferred to the flow of liquid because of an outer insulation of Fiberglass. Thermocouples, which were mounted between the copper tube and nichrome tape at intervals of about 100 mm in the direction of flow and in upstream and downstream mixing boxes, were used for the measurements of wall and liquid temperatures. Temperature differences between the inlet and outlet and those between the wall and bulk were within 5°C to avoid natural convection as far as possible.

Measurements of longitudinal pressure drop of the flows were made by using pressure taps with a pressure transducer. These taps were located in the upstream and downstream headers, where there was no direct effect of electric field.

The test liquids were castor oil ($\mu \cong 100$ cP, $Pr \cong 2000$), silicone oil ($\mu \cong 10$ cP, $Pr \cong 100$) and turpentine oil ($\mu \sim 1.35$ cP, $Pr \cong 20$), and experiments were conducted at room temperature.

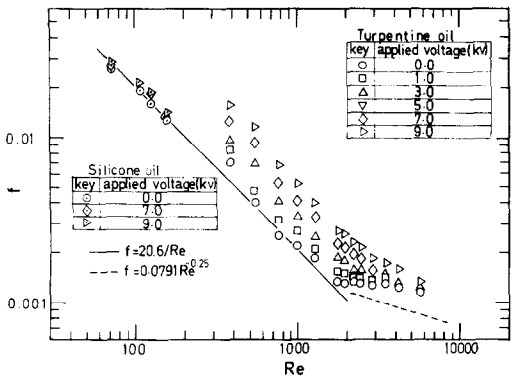

FIG. 2. Change of friction factor with voltage applied.

Profiles of temperature and velocity were measured by using a thermocouple probe (Chromel–Almel sheathed on the inside by stainless steel of 0.25 mm O.D. and outside by vinyl of 1.3 mm O.D. and 50 mm length) and a total pressure tube (glass tube of 1.5 mm O.D. and 50 mm length) in the test liquid of silicone oil. Traversing devices were installed in another test heat exchanger, the diameter of which was twice as large as that shown in Fig. 1. Measurements of temperature and velocity profile were conducted at the position of 1350 mm from the inlet.

3. EXPERIMENTAL RESULTS AND DISCUSSIONS

3.1. *Heat-transfer coefficient and longitudinal pressure drop*

Figure 2 shows pressure drop results in isothermal flow at about 20°C in terms of conventional Fanning's friction factor f. The error of the measured pressure drop due to the end effect was estimated to be within 15%. The changing behaviour at the same voltage applied is different for the silicone and turpentine oils. For the silicone oil, the change in the friction factor with applied voltage is small. But for the turpentine oil the friction factors increase with applied voltage and correlation lines of f for each value of applied voltage are parallel to that without electric field in the region of laminar flow. In the turbulent region, the results for turpentine oil show that the changes caused by electric field become gradually small with increasing Reynolds number. Data for castor oil are omitted in Fig. 2, because they fall in the range of $1 < Re < 10$ and no variation of f with the voltage up to 9 kV was observed at isothermal conditions. This difference of the changing behaviour for the castor, silicone and turpentine oils may be due to difference of viscosity for those oils as discussed in Section 3.3. During heat transfer under the electric field, friction factors increased with voltage, because the viscosity increased with decreasing liquid temperature near the outer wall due to an increasing heat transfer coefficients.

Nusselt numbers at the outer wall of the annulus in the laminar region are correlated with Graetz number in Fig. 3(a) for the castor oil, Fig. 3(b) for silicone oil and Fig. 3(c) for turpentine oil. The value of Nu without electric field is somewhat high in comparison with that calculated on the condition of well-developed laminar flow depicted by dot-dashed curve in Figs. 3(a–c), probably because the flow conditions are not fully developed. Under the electric field, Nusselt numbers of all three liquid flows are markedly increased at a larger Graetz number region, and for each liquid these values seem to remain constant for each value of voltage applied. However, at a smaller Graetz number region the values of Nu are the same both with and without electric field. From these results we can imagine that electroconvection hardly disturbs flow very near the wall.

Figure 4(a) shows the change of Nusselt number for the turpentine oil with longitudinal distance for various Reynolds numbers in the case without electric field. The dip in the curves at Reynolds number larger than 2860 may be explained by the fact that the boundary layers along the tube walls are at first laminar and change through a transition region to turbulent flow. Figures 4(b), 4(c) and 4(d) show those for

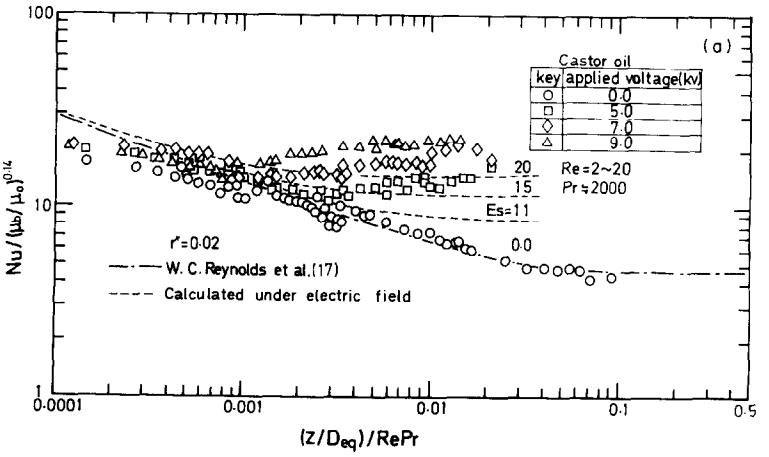

FIG. 3(a)

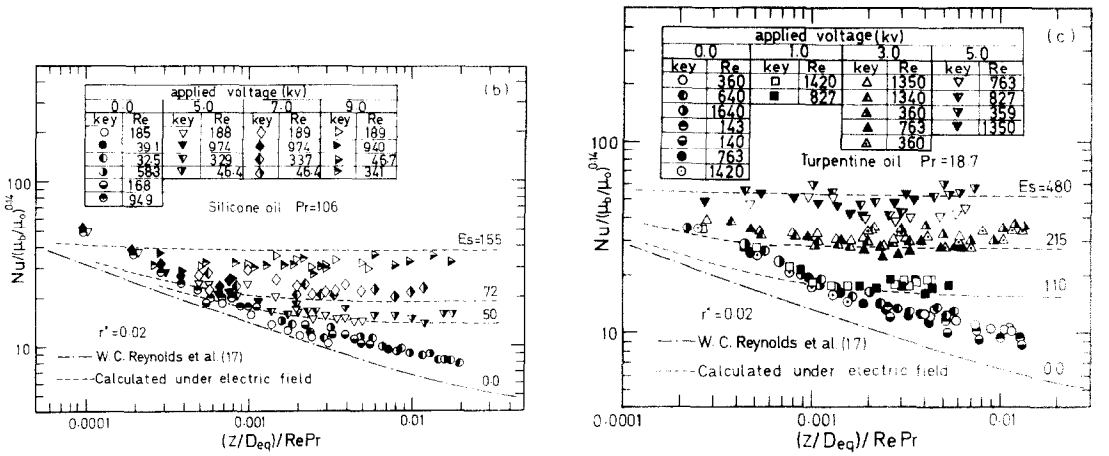

FIG. 3(a–c). Change of Nusselt numbers for (a) castor oil (b) silicone oil and (c) turpentine oil with voltage applied at laminar range of Reynolds number.

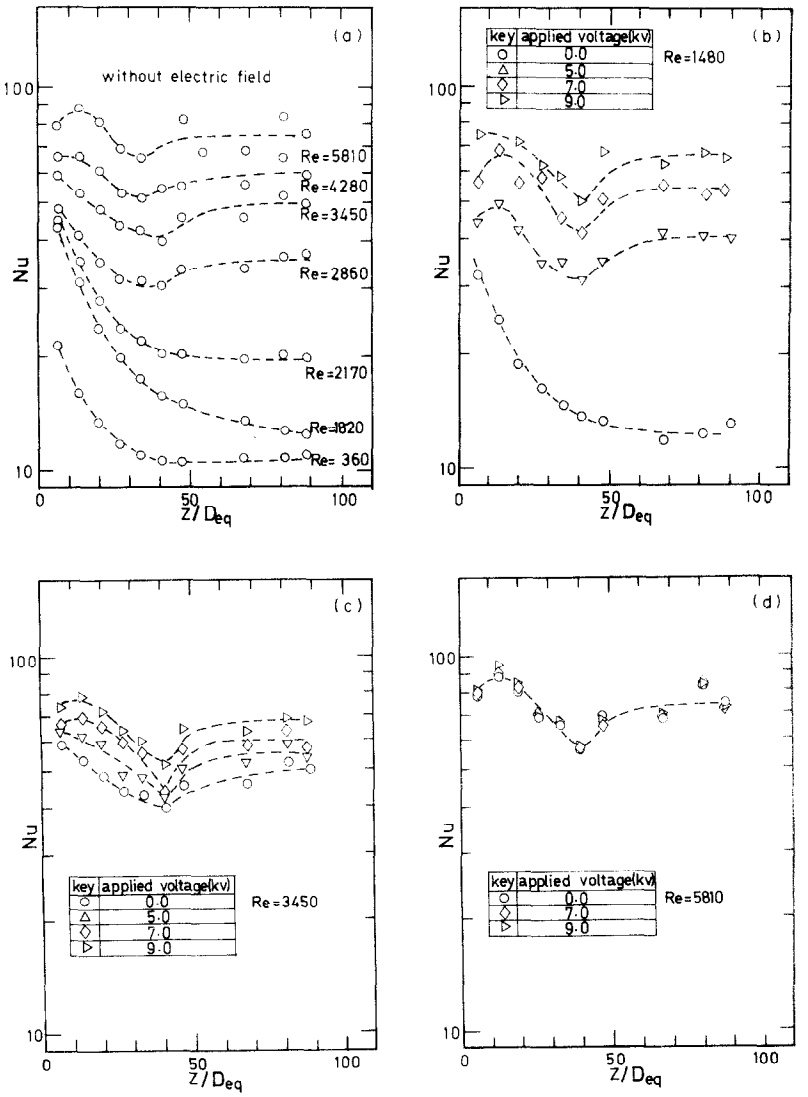

FIG. 4(a–d). Change of Nusselt number for (a) turpentine oil with Reynolds number, (b) voltage applied at laminar, (c) transitional and (d) turbulent range of Reynolds number.

various applied voltage at $Re = 1480$, 3450 and 5810, respectively. From the figures it can be seen that the effect of increasing applied voltage on Nusselt number resembles that of the increase of Reynolds number.

3.2. *Equations of change under an electric field*

When a fluid containing electric charge is subjected to an electric field, the change in density of space-charge and strength of electric field, and the conservation of mass, momentum and heat are expressed with dimensionless representations as

$$\frac{DN}{D\tau} = -\left(\frac{I_o r_o^3 \rho}{\mu^2 b^*}\right)^{1/2}\left(\frac{\rho b^{*2}}{\varepsilon}\right) \times \nabla\cdot N\mathbf{F} + \left(\frac{\mathscr{D}^*\rho}{\mu}\right)\nabla^2 N \quad (1)$$

$$\nabla\cdot\mathbf{F} = N \quad (2)$$

$$\nabla\cdot\mathbf{v} = 0 \quad (3)$$

$$\frac{D\mathbf{v}}{D\tau} = -\nabla P + \nabla^2\mathbf{v} + \left(\frac{I_o r_o^3 \rho}{\mu^2 b^*}\right)N\mathbf{F} \quad (4)$$

$$\frac{D\Theta}{D\tau} = \left(\frac{\lambda}{c_p\mu}\right)\left\{\nabla^2\Theta + \left[\frac{r_o I_o}{q_o}\left(\frac{I_o r_o}{\varepsilon b^*}\right)^{1/2}\right] \times \left[N\mathbf{F}\cdot\mathbf{F} + \left(\frac{\mathscr{D}^*\rho}{\mu}\right) \times \left(\frac{I_o r_o^3\rho}{\mu^2 b^*}\right)^{-1/2}\left(\frac{\rho b^{*2}}{\varepsilon}\right)^{-1/2}\mathbf{F}\cdot\nabla N\right]\right\} \quad (5)$$

where

$$N = en(r_o b^*/I_o\varepsilon)^{1/2}, \quad \mathbf{F} = \mathbf{E}(\varepsilon b^*/I_o r_o)^{1/2},$$
$$\mathbf{v} = \mathbf{u}r_o\rho/\mu, \quad P = pr_o^2\rho/\mu^2,$$
$$\Theta = (T - T_e)\lambda/q_o r_o, \quad \tau = t\mu/\rho r_o^2,$$
$$\nabla = r_o\nabla,$$

where r_o is a reference distance, I_o is electric current density at r_o, q_o is a heat flux at r_o. In these equations, the following assumptions are made. (1) Fluid properties are constant. (2) As suggested by Stuetzer [1], fluxes of electric charges of various kinds of species are replaced by a flux of one kind of space-charge, that is

$$\sum_i \mathbf{I}_i = \sum_i (b_i^* e n_i\mathbf{E} + \mathscr{D}_i\nabla e n_i + \mathbf{u}e n_i) = b^* en\mathbf{E} + \mathscr{D}^*\nabla en + \mathbf{u}en = \mathbf{I} \quad (6)$$

where the mobility b^* and diffusivity $\mathscr{D}^*$ are averaged values. This assumption leads to equation (1). (3) Electrostrictive and gravitational forces can be omitted in equation (4). (4) The viscous heating term can be neglected in equation (5).

As is seen from equation (4), the Coulomb force $(I_o r_o^3\rho/\mu^2 b^*)N\mathbf{F}$ contributes to a change in fluid motion, and consequently to a change in the mechanism of heat transfer through the convection term and the joule heating effect.

To give some insight into the electrical feature governing the Coulomb force, further assumptions are made. (5) The variation of electrical field in axial direction can be neglected in comparison with that in radial direction, because the present study concerns with the flow of dielectric organic liquids in a long concentric cylindrical system in which a constant electric potential is applied between the inner and outer walls. (6) Because of sufficiently large values of $(I_o r_o^3\rho/\mu^2 b^*)^{1/2}$ $(\rho b^{*2}/\varepsilon)$ in the present experimental runs, the migrations of space-charge due to diffusion and bulk convection are assumed to be negligibly small in comparison with that due to electric field.

Thus,

$$0 = \frac{1}{r}\frac{\partial}{\partial r}(rNF_r) \quad (7)$$

$$\frac{1}{r}\frac{\partial}{\partial r}(rF_r) = N. \quad (8)$$

The above two equations show that the quantity NF_r is solved as a simple function of r when the conditions imposed on N at the walls are given. One of the conditions is that $rNF_r = 1$ at the outer wall. However, the second condition is not known because of little knowledge on the exact electric phenomena occurring in the fluid near the inner wall where the strength of the electric field is very large. According to the Poole–Frenkell effect, the density of the space-charge increases rapidly with increasing electric field strength. Therefore, near the inner wall a hypothetical radial position $r_\#$ where $N = N_\#$ is assumed.

Thus, the following equation is obtained.

$$F_r^2 = 1 + \frac{1}{r^2}\left(\frac{1}{N_\#^2} - r_\#^2\right). \quad (9)$$

Equation (9) gives $F_r \approx -1$ at $r \gg r^*$ because the value of $N_\#$ is large and $r_\# \approx r^*$. On the other hand, the relation $\nabla V = -\mathbf{E}$ gives the potential drop between the walls as

$$\frac{V_o - V_i}{(I_o r_o^3/\varepsilon b^*)^{1/2}} = -\int_{r^*}^{1} F_r\,\mathrm{d}r \quad (10)$$

The integral on the right hand side of equation (10) is divided into two regions of $r^* \le r \le r_\#$ and $r_\# \le r \le 1$, and substitution of equation (9) at $r_\# \le r \le 1$ gives the following equation for potential drop.

$$(V_o - V_i) = (V_\# - V_i) + \left(\frac{I_o r_o^3}{\varepsilon b^*}\right)^{1/2}\beta \quad (11)$$

where

$$(V_\# - V_i) = \left(\frac{I_o r_o^3}{\varepsilon b^*}\right)^{1/2}\int_{r^*}^{r_\#}(-F_r)\mathrm{d}r$$

and

$$\beta = \int_{r_\#}^{1}(-F_r)\mathrm{d}r.$$

Equation (11) suggests a linear relation between $(V_o - V_i)$ and $(I_o r_o^3/\varepsilon b^*)^{1/2}$ when $(V_\# - V_i)$ and β are constant. In fact, the value of β can be expected to be an

order of magnitude of unity from the description related to equation (9). In an experiment with air flow, the linear relation holds satisfactorily at high values of $(V_o - V_i)$, and the slope and intercept depend only on the geometrical factor, independent of the flow conditions; $(V_\# - V_i)$ depends mainly on (r_i/r_o) and β on (l/r_o). The dependency of β on l/r_o may arise from the end effect in measuring the electrical current [12]. In the present liquid system relations between the voltage difference $(V_o - V_i)$ and total current through the outer wall $(I = 2\pi r_o l I_o)$ are shown in Figs. 5(a) and 5(b). Solid lines in these figures show linear approximations indicating that β in the equation (11) is constant, although the validity of the linear approximation at small values of $(V_o - V_i)$ is lost, probably because convection and diffusion effects cannot be neglected.

From equation (7) the Coulomb force $(I_o r_o^3 \rho/\mu^2 b^*)$ NF_r is found to be characterized by only one dimensionless complex $Es = (I_o r_o^3 \rho/\mu^2 b^*)^{1/2}$. This means that the flow characteristics in the electric field are determined by Reynolds number and Es. However, in calculating the dimensionless complex Es, it is necessary to know the exact value of b^* which is often difficult to obtain. Therefore, it is convenient to rewrite Es with empirical value of $V_\#$ and β as follows.

$$Es = \left(\frac{I_o r_o^3 \rho}{\mu^2 b^*}\right)^{1/2} \cong \frac{(V_o - V_\#)\varepsilon^{1/2}\rho^{1/2}}{\mu^2 \beta} \qquad (12)$$

In this equation, use is made of the equation (11), and the result obtained in air flow, that β is function of only (l/r_o), is implicitly assumed to apply in any flow. In fact, in the present liquid flows the value of b^* is not known. Therefore we adopt a slightly modified value of β obtained in air flow in correlating the experimental results as shown in a subsequent section. Difference in the value of β due to the electrodes shape is examined in flows of silicone oil as shown in Fig. 5(b). From the slope of lines in Fig. 5(b) the value of β in the larger tube system $(l/r_o = 96.6)$ is taken as 0.71 times that in the smaller one $(l/r_o = 187)$, because the ionic mobility and dielectric constant are same.

When the value of applied voltage $(V_o - V_i)$ is small, equation (12) does not hold as discussed above. However, if we assume that the mobility b^* calculated

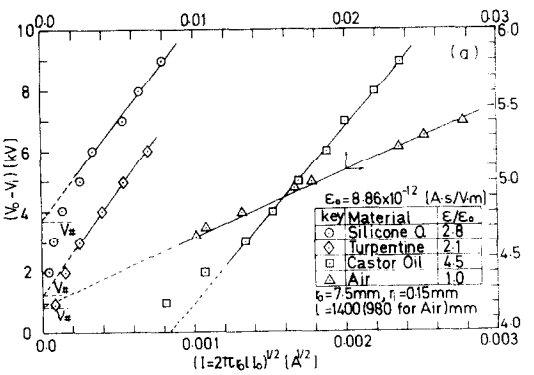

FIG. 5(a). Change of electric current through outer wall with voltage applied between electrodes.

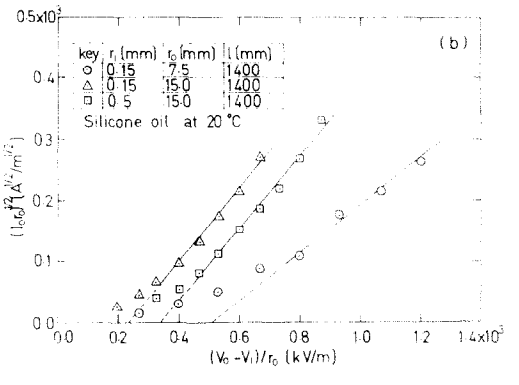

FIG. 5(b). Variation of relation between electric current through outer wall and voltage applied with geometrical factor of electrodes in silicone oil.

by using measured relation between $I_o^{1/2}$ and $(V_o - V_i)$ for high applied voltage conditions can be used in this low voltage conditions, we can determine the value of Es.

The joule heating $[r_o I_o/q_o(I_o r_o/\varepsilon b^*)^{1/2}]$ which appears in the equation (5) is evaluated to be less than 5×10^{-4} in the heat transfer experiments presented in the previous section. These are negligibly small in the heat balance of the present liquid system, because of a sufficiently large value of q_o.

3.3. *Calculations of Nusselt number and longitudinal pressure drop*

We can not give exact solutions of the basic equations presented above. However, we intend to give some systematic discussions for relations between the changes of Nusselt number and longitudinal pressure drop under the effect of radial electric potential.

When we deal with a well-developed flow at a steady-state, any direct force due to a radial electric field does not appear in a longitudinal momentum balance, and also the radial force contributes only to a radial pressure distribution, if radial and circumferential velocity components are negligible. However, from the practical existence of radial current caused by the movements of ions, it is reasonable to assume that radial velocity exists, although it is small. Then, a momentum flux due to the radial velocity component should not be ignored in the longitudinal momentum balance, nor a heat flux in a heat balance.

For these fluxes we will apply diffusivities of momentum and heat due to the electric field, similar to turbulent flow, and will start by assuming momentum and heat balances as

$$\frac{dP}{dz} = \frac{1}{r}\frac{d}{dr}\left\{r\left(-\overline{v_z' v_r'} + \frac{d\bar{v}_z}{dr}\right)\right\} = \frac{1}{r}\frac{d}{dr}\left\{r\left(1 + \frac{\varepsilon_M}{\nu}\right)\frac{d\bar{v}_z}{dr}\right\} \qquad (13)$$

$$Pr\,\bar{v}_z\frac{\partial\bar{\Theta}}{\partial z} = \frac{1}{r}\frac{\partial}{\partial r}\left\{r\left(-Pr\,\overline{v_r'\Theta'} + \frac{\partial\bar{\Theta}}{\partial r}\right)\right\} = \frac{1}{r}\frac{\partial}{\partial r}\left\{r\left(1 + Pr\frac{\varepsilon_H}{\nu}\right)\frac{\partial\bar{\Theta}}{\partial r}\right\} \qquad (14)$$

with boundary conditions for longitudinal velocity

$$\overline{v_z(r)}\Big|_{r=1} = \overline{v_z(r)}\Big|_{r=r^*} = 0 \tag{15}$$

and for temperature

$$\overline{\Theta(z,r)}\Big|_{z=0} = 0, \qquad \frac{\partial}{\partial r}\overline{\Theta(z,r)}\Big|_{r=1} = -1$$

and

$$\frac{\partial}{\partial r}\overline{\Theta(z,r)}\Big|_{r=r^*} = 0, \tag{16}$$

where $\overline{A(z,r)}$ means time-averaged value, i.e. $A(z,r,t) = \overline{A(z,r)} + A'(z,r,t)$. Hereafter the over-bar will be omitted.

The solution of equation (13) satisfying equation (15) is

$$\frac{v_z}{\langle v_z\rangle} = \tfrac{1}{2}C_1 \int_{r^*}^{r} \frac{r^2 + C_2}{r(1+\varepsilon_M/\nu)}\,\mathrm{d}r \tag{17}$$

where

$$\langle v_z\rangle = \int_{r^*}^{1} v_z r\,\mathrm{d}r \Big/ \int_{r^*}^{1} r\,\mathrm{d}r, \tag{18}$$

$$C_1 = \frac{\mathrm{d}P}{\mathrm{d}z}\frac{1}{\langle v_z\rangle} = -2(1-r^{*2}) \Big/ \int_{r^*}^{1} \frac{r(r^2+C_2)}{1+\varepsilon_M/\nu}\,\mathrm{d}r$$

and

$$C_2 = -\int_{r^*}^{1} \frac{r^2}{r(1+\varepsilon_M/\nu)}\,\mathrm{d}r \Big/ \int_{r^*}^{1} \frac{1}{r(1+\varepsilon_M/\nu)}\,\mathrm{d}r.$$

The friction factor and Reynolds number are expressed as

$$f = \frac{1-r^*}{C_1\langle v_z\rangle} \tag{19}$$

$$Re = 2(1-r^*)\langle v_z\rangle \tag{20}$$

From equations (14) and (16) the temperature change is obtained as

$$\Theta\left(\frac{z}{Pr\langle v_z\rangle}, r\right) = \Theta_{\infty z}\left(\frac{z}{Pr\langle v_z\rangle}\right) + \Theta_{\infty r}(r) + \sum_{n=1}^{\infty} A_n \exp\left(-\lambda_n^2 \frac{z}{Pr\langle v_z\rangle}\right) R_n(r), \tag{21}$$

where $\Theta_{\infty z} + \Theta_{\infty r}$ is a solution of equation (14) satisfying the conditions;

$$\frac{\mathrm{d}}{\mathrm{d}r}\Theta_{\infty r}(r)\Big|_{r=1} = -1, \qquad \frac{\mathrm{d}}{\mathrm{d}r}\Theta_{\infty r}(r)\Big|_{r=1} = 0$$

$$\frac{z}{Pr\langle v_z\rangle} + \int_{r^*}^{1}\left\{\Theta_{\infty z}\left(\frac{z}{Pr\langle r_z\rangle}\right) + \Theta_{\infty r}(r)\right\} \times \frac{v_z}{\langle v_z\rangle} r\,\mathrm{d}r = 0, \tag{22}$$

and λ_n and $R_n(r)$ are eigenvalues and eigenfunctions, respectively, satisfying the following differential equation and boundary conditions;

$$\frac{1}{r}\frac{\mathrm{d}}{\mathrm{d}r}\left\{r\left(1 + Pr\frac{\varepsilon_H}{\nu}\right)\frac{\mathrm{d}R_n}{\mathrm{d}r}\right\} + \lambda_n^2 \frac{v_z}{\langle v_z\rangle} R_n = 0 \tag{23}$$

$$\frac{\mathrm{d}}{\mathrm{d}r}R_n(r)\Big|_{r=1} = \frac{\mathrm{d}}{\mathrm{d}r}R_n(r)\Big|_{r=r^*} = 0,$$

and A_n is given by the following equation;

$$A_n = \int_{r^*}^{1} \{\Theta_{\infty z}(0) + \Theta_{\infty r}(r)\} R_n(r) \frac{v_z}{\langle v_z\rangle} r\,\mathrm{d}r \Big/ \int_{r^*}^{1} \{R_n(r)\}^2 \frac{v_z}{\langle v_z\rangle} r\,\mathrm{d}r \tag{24}$$

The bulk temperature is derived from the heat balance as

$$\Theta_b\left(\frac{z}{Pr\langle v_z\rangle}\right) = \frac{(T_b - T_e)\lambda}{q_o r_o} = \frac{2}{(1-r^*)}\frac{z}{Pr\langle v_z\rangle}, \tag{25}$$

and then Nusselt number and Graetz number are

$$\frac{1}{Nu} = \frac{(T_b - T_o)\lambda}{q_o De_q} = -\left\{\Theta_b\left(\frac{z}{Pr\langle v_z\rangle}\right) + \Theta\left(\frac{z}{Pr\langle v_z\rangle}, 1\right)\right\} \Big/ 2(1-r^*) \tag{26}$$

$$Gz = (z/De_q)/RePr = 4(1-r^*)\frac{z}{Pr\langle v_z\rangle}. \tag{27}$$

After the calculation of the velocity profile, the eigenvalues and eigenfunctions can be easily obtained numerically by the method of Berry and de Prima [18], and then the Nusselt number is calculated.

For the diffusivities which have to be determined empirically, a simple model has been proposed for an air system in a previous paper [12], where the flow is divided into two regions of core and viscous layer near the outer wall, and the values of diffusivities are assumed to be constant in the core region and zero near the wall. However, this model, similar to Prandtl's analogy between heat and momentum transfer in turbulent flow, is not appropriate in the liquid system, because Prandtl number significantly differs from unity. For the present discussion, a radial distribution of momentum diffusivity of fully developed turbulent flow in a circular tube will be assumed as a clue. That is

$$\frac{\varepsilon_M}{\nu} \cong 0.4 r_o^+ (1-r)\left\{1 - \exp\left[-\frac{r_o^+}{26}(1-r)\right]\right\}^2$$

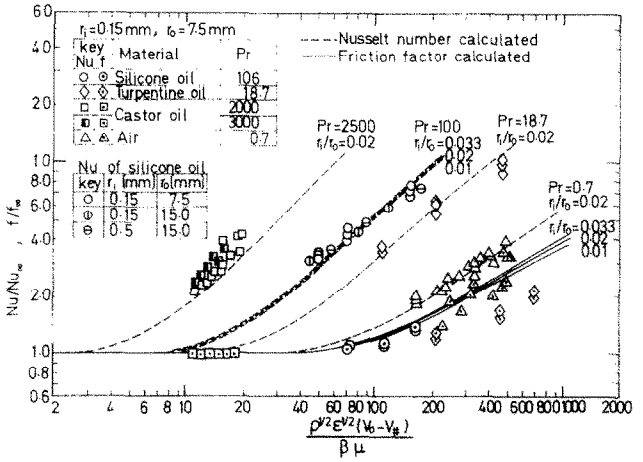

FIG. 6. Correlations of Nu and f in thermally well developed laminar range of Reynolds number with electric field.

Taking into account an inner wall effect and further supposing that r_o^+ is a function of Es^n, we presume that momentum diffusivity is modeled as

$$\frac{\varepsilon_M}{\nu} = 0.4Es^n(1-r) \times \left\{1-\exp\left[-\frac{1}{26}Es^n(1-r)\right]\right\}^2 \times (r-r^*)\left\{1-\exp\left[-\frac{1}{26}Es^n(r-r^*)\right]\right\}, \tag{28}$$

and the diffusivity of heat as

$$\frac{\varepsilon_H}{\nu} = \sigma\frac{\varepsilon_M}{\nu}, \tag{29}$$

where n and σ are empirical constants.

The results calculated by choosing $n = 0.8$ and $\sigma = 1.5$ at a thermally well developed region, where the Graetz number has a negligible effect, are compared with the experimental results in Fig. 6. Nu_∞ and f_∞ of the ordinate of this diagram denote the theoretical values at fully developed laminar condition without electric field. For the abscissa, the empirical relation of equation (12) was used with the assumption of $\beta = 0.7$, which is a slightly modified value of the empirical relation in the air system, $\beta = 0.5$, in which the ionic mobility is known. The present calculation gives good predictions for the experimental characteristic of liquids of large Prandtl number that the change of longitudinal pressure drop is negligibly small, but that the change of heat transfer rate is remarkable.

In the data of silicone oil, the results of the larger test tube in which two kinds of inner wires are used are also plotted. The direct effect of inner and outer diameters is found to be small experimentally and analytically as shown in Fig. 6. The calculated results at thermally developing region are depicted in Fig. 3 by dashed lines to compare with the experimental results. However, it should be noted that the flow conditions at small Graetz number region in the present experiment were not fully developed, whereas the calculation was performed on the assumption of fully developed flow condition.

3.4. *Temperature profile and flow behaviour*

The temperature profiles measured in the silicone oil are shown in Fig. 7 along with the calculated curves. Under the application of electric field, the temperature profile becomes flatter in the core and sharper at the wall due to the convection induced by the electric field.

The experimental results of velocity profile in the silicone oil at constant temperature are compared with the calculated results in Fig. 8. Although the experimental velocity profile in Fig. 8 is not as accurate as the

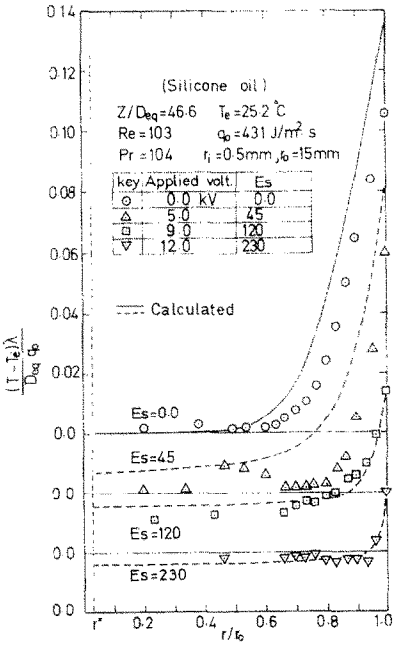

FIG. 7. Temperature profile in flow of silicone oil under electric field.

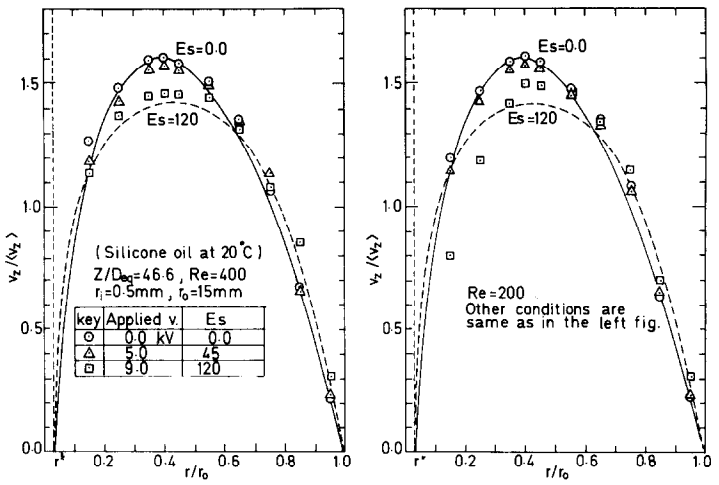

FIG. 8. Velocity profile in flow of silicone oil under electric field.

temperature profile in Fig. 7 owing to the difficulty in measuring the low velocity, one can see that it becomes flatter when the electric field is applied. It is also seen that the deformation of the velocity profile in liquid flow under the electric field is not as large as that in the air flow shown in Fig. 9.

4. CONCLUSIONS

Experimental investigations of heat and momentum transfers in the flow of dielectric organic liquids inside annuli between the inner wire and outer copper tube under an electric field were conducted and the following conclusions were obtained.

1. In the laminar flow range, the increase of Nusselt number and friction factor are induced by contributions of radial convection owing to movements of space-charge.
2. For a high Prandtl number liquid, Nusselt number increase much more than the increase of friction factor.
3. These contributions to heat transfer are small in the turbulent flow and also at the thermal entrance region of laminar flow.

Empirical formulation using the electroconvective diffusivities of equations (28) and (29) gives satisfactory representations for the both changes of Nusselt number and the friction factor in the laminar range, when the empirical relation of equation (12) between the electric current density and voltage is used as the electroconvective parameter. Further analyses of the temperature and velocity profiles are necessary.

Acknowledgements—This study is indebted to Grant in Aid for Scientific Research, project number 185208, of the Ministry of Education, Japan. The authors wish also to thank undergraduate students Messrs K. Sato and N. Nagasaki for their help in construction of equipments and numerous measurements.

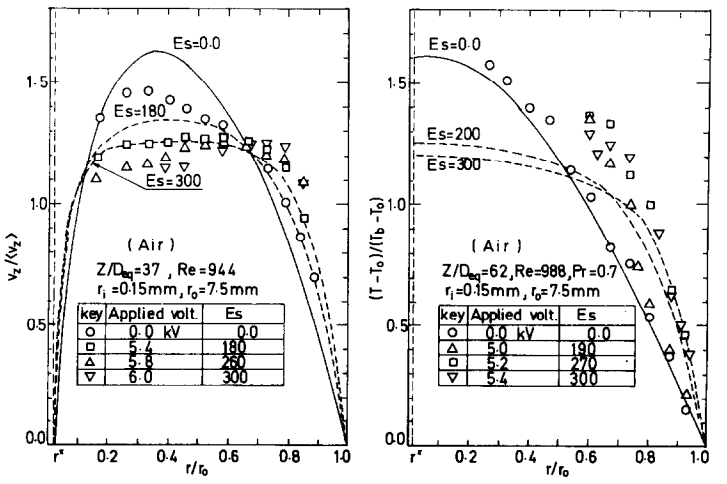

FIG. 9. Temperature and velocity profiles in flow of air under electric field.

REFERENCES

1. O. M. Stuetzer, Ion drag pressure generation, *J. Appl. Phys.* **30,** 984 (1959).
2. O. M. Stuetzer, Magnetohydrodynamics and electrohydrodynamics, *Physics Fluids* **5,** 534 (1962).
3. H. Senftleben, Die Einwirkung elektrisher und magnetisher Felder auf des Wärmeleitvermögen von Gasen, *Phys. Z.* **32,** 550 (1931).
4. R. Kronig and N. Schwarz, On the theory of heat transfer from a wire in an electric field, *Appl. Scient. Res.* **A1,** 35 (1947).
5. M. E. Frank, Effect of vortices induced by corona discharge on free-convection heat transfer from a vertical plate, *J. Heat Transfer* **91,** 427 (1969).
6. A. Yabe, Y. Mori and K. Hijikata, EHD study of the corona wind between wire and plate electrodes, *AIAA J.* **16,** 340 (1978).
7. H. Konno, M. Kuriyama, M. Asano and E. Harada, Heat transfer from circular pipes under corona discharge, *Kagaku Kogaku Ronbunshu* **4,** 366 (1978).
8. R. A. Moss and J. Grey, Heat transfer augmentation by steady and alternative electric fields, *Proc. Heat Transfer Fluid Mech. Inst.*, p. 210, Stanford University Press, Palo Alto (1966).
9. B. R. Lazarenko, F. P. Grosu and M. K. Bologa, Convective heat-transfer enhancement by electric fields, *Int. J. Heat Mass Transfer* **18,** 1433 (1975).
10. S. E. Sadek, R. G. Fox and M. Hurwitz, The influence of electric fields on convective heat and mass transfer from a horizontal surface under forced convection, *J. Heat Transfer* **94,** 144 (1972).
11. H. R. Velkoff and R. Godfrey, Low-velocity heat transfer to a flat plate in the presence of a corona discharge in air, *J. Heat Transfer* **101,** 157 (1979).
12. T. Mizushina, H. Ueda, T. Matsumoto and K. Waga, Effect of electrically induced convection on heat transfer of air flow in an annulus, *J. Chem. Engng Japan* **9,** 72 (1976).
13. M. Robinson, Convective heat transfer at the surface of a corona electrode, *Int. J. Heat Mass Transfer* **13,** 263 (1970).
14. E. Schmidt and W. Leidenfrost, Der Einfluss elektrisher Felder auf den Wärmetransport in Flussigen elektrisher Nichtleitern, *Forsch. Geb. IngWes* **19,** 65 (1953).
15. J. E. Porter and R. Poulter, Electrically induced convection accompanying laminar flow heat transfer in an annulus, CHMECA'70 Melbourne and Sydney 19-26 August, 1970, The Institution of Chemical Engineers Symposium Series No. 33, Session 6A, 34 (1970).
16. J. E. Porter and R. B. Smith, The effect of a transverse electrostatic field on laminar flow heat transfer in a rectangular duct, *Proc. 5th Int. Heat Trans. Conference* Paper FC 5.4 A.I.Ch.E., New York (1974).
17. R. E. Lundberg, P. A. McCuen and W. C. Reynolds, Heat transfer in annular passages. Hydrodynamically developed laminar flow with arbitrarily prescribed wall temperatures or heat flux, *Int. J. Heat Mass Transfer* **6,** 495 (1963).
18. V. J. Berry and C. R. de Prima, An iterative method for the solution of eigenvalue problems, *J. Appl. Phys.* **23,** 195 (1952).

EFFET D'UN CHAMP ELECTRIQUE RADIAL SUR LES TRANSFERTS DE CHALEUR ET DE QUANTITE DE MOUVEMENT DANS UN LIQUIDE DIELECTRIQUE ORGANIQUE EN ECOULEMENT LAMINAIRE DANS UN ESPACE ANNULAIRE

Résumé—Des expériences ont pour but d'étudier les changements dans le transfert convectif de chaleur dans des écoulements de liquides diélectriques organiques à l'intérieur d'un espace annulaire entre un tube de cuivre et un fil concentrique. Est aussi mesurée la chute de pression longitudinale dans l'écoulement qui peut être induit par l'application de champ électriques de courant continu entre la paroi du tube et l'électrode centrale. Dans le domaine laminaire, le flux de chaleur à la paroi externe augmente dans la région bien établie et l'établissement thermique est avancé. D'autre part, les chutes de pression sont augmentées dans des liquides à faible nombre de Prandtl. Dans les domaines de transition et turbulent, néanmoins, on ne note pas de changements de transferts thermique et de quantité de mouvement. Pour exprimer ces résultats dans le domaine des faibles nombres de Reynolds, on donne une formulation semi-empirique en termes adimensionnels à partir du principe de similarité.

DER EINFLUß EINES RADIALEN ELEKTRISCHEN FELDES AUF DEN WÄRME- UND IMPULSAUSTAUSCH IN DIELEKTRISCHEN ORGANISCHEN FLÜSSIGKEITEN, WELCHE LAMINAR DURCH EINEN KONZENTRISCHEN RINGRAUM STRÖMEN

Zusammenfassung—Experimentell untersucht wurde der konvektive Wärmeübergang dielektrischer organischer Flüssigkeiten im Ringraum zwischen einem Kupferrohr und konzentrischen Drähten. Darüber hinaus wurde der Druckabfall längs des Rohres gemessen, welchen man durch Anlegen einer Gleichspannung zwischen Rohrwand und konzentrischem Draht erzeugen konnte. Bei laminarer Strömung nahm der Wärmestrom im thermisch ausgebildeten Bereich zu, und die thermische Ausbildung wurde gefördert. Auf der anderen Seite nahm auch der Druckabfall bei Flüssigkeiten mit kleinen Prandtl-Zahlen zu. Im Übergangsbereich sowie im Bereich der turbulenten Strömung änderten sich weder der Wärme- noch der Impulsaustausch. Um bei kleinen Reynolds-Zahlen die Versuchsergebnisse darstellen zu können, wurde auf der Grundlage der Ähnlichkeitstheorie eine halbempirische Gleichung in dimensionsloser Schreibweise abgeleitet.

ВЛИЯНИЕ РАДИАЛЬНОГО ЭЛЕКТРИЧЕСКОГО ПОЛЯ НА ПЕРЕНОС ТЕПЛА И КОЛИЧЕСТВА ДВИЖЕНИЯ В ДИЭЛЕКТРИЧЕСКОЙ ОРГАНИЧЕСКОЙ ЖИДКОСТИ ПРИ ЛАМИНАРНОМ ТЕЧЕНИИ В КОНЦЕНТРИЧЕСКИХ КОЛЬЦЕВЫХ КАНАЛАХ

Аннотация — Проведено экспериментальное исследование конвективного теплопереноса при течении диэлектрической органической жидкости в кольцевом зазоре между медной трубкой и коаксиальным электродом. Исследовался также продольный перепад давления в потоке, возникающий при наложении постоянного электрического поля между стенкой трубки и электродом. В ламинарном диапазоне значений числа Рейнольдса интенсивность переноса тепла к внешней стенке возрастала в области полностью развитого теплообмена. С другой стороны, наблюдалось увеличение перепада давления в жидкости с низкими значениями числа Прандтля. Однако, в переходном и турбулентном диапазонах *Re* не наблюдалось изменений ни в количестве тепла, ни в количестве движения. Для пересчета этих результатов на диапазон низких значений числа Рейнольдса выведена полуэмпирическая формула в безразмерном виде, исходя из принципа автомодельности.